Rea, D.K., Basov, I.A., Scholl, D.W., and Allan, J.F. (Eds.), 1995
Proceedings of the Ocean Drilling Program, Scientific Results, Vol. 145

3. HIGH-RESOLUTION DIATOM PALEOCLIMATOLOGY OF THE MIDDLE PART OF THE PLIOCENE OF THE NORTHWEST PACIFIC[1]

John A. Barron[2]

ABSTRACT

The relative abundance of diatom taxa is tabulated for northwestern Pacific Ocean Drilling Program Sites 881 and 883 during a climatically warm interval of the middle part of the Pliocene (~3.4–3.1 Ma). The records of both sites are well constrained by magnetostratigraphy. Sample spacing averages 10.5 k.y. for Site 881 and between 3 and 4 k.y. for Site 883.

At Site 881, relative abundance values of the modern subtropical diatom *Hemidiscus cuneiformis* rise to about 10%–20% of the diatom assemblage during the same 3.20 to 3.08 Ma interval (Subchron C2An.2n to lower C2Ar.1r) when maximum values (13%–35%) of this same taxon are documented at Deep Sea Drilling Program Site 580 to the south. The middle Pliocene diatom assemblages of Site 883, however, are strongly subarctic in character, based on the consistent dominance (60%–85%) of *Neodenticula kamtschatica.*

Two paleoclimate ratios, *Twt* and Td_f, are used at Sites 580, 881, and 883 to estimate mid-Pliocene sea surface temperatures (SST). The *Twt* ratio compares the number of modern and Pliocene subtropical and tropical diatoms to cooler water (subarctic and cool-transitional) taxa with warm-transitional taxa factored into the equation at a value of one half. *Twt* ratios in modern northwest Pacific core-top assemblages show a strong linear relationship with February SST ($R^2 = 0.807$), while the relationship with August SST is weaker ($R^2 = 0.594$).

The Td_f ratio is proposed, where $Td_f = (X_{Nr} + 0.5 \times \{X_{Tn}\})/(X_{Nr} + X_{Tn} + X_{Neo})$ and X_{Nr} = *Nitzschia reinholdii* s. ampl., X_{Tn} = *Thalassionema nitzschioides,* and X_{Neo} = the total *Neodenticula* spp. For modern core-top data, the Td_f ratio displays a strong linear relationship with both February and August SST data ($R^2 = 0.888$ and 0.736, respectively).

Predicted differences of mid-Pliocene February SSTs above modern values are +7°C (*Twt*) vs. +4°C to +5°C (Td_f) at Site 580 and +6°C (*Twt*) vs. 0°C to +3°C (Td_f) at Site 881; both ratios predict little change from modern conditions at Site 883. August SST anomalies are estimated to have been +2°C to +3°C at Site 580 for both paleoclimate ratios; +6°C (*Twt*) vs. +2°C to +3°C (Td_f) at Site 881; and +5°C (*Twt*) vs. +4°C (Td_f) at Site 883.

INTRODUCTION

Investigation of a climatically warm interval centered at 3.0 Ma (age according to the Berggren et al. [1985] time scale) is a major goal of the Pliocene Research, Interpretations, and Synoptic Mapping Project (PRISM) of the U.S. Geological Survey, which aims to reconstruct global environmental conditions during a Pliocene warm interval before the onset of Northern Hemisphere glaciation (Cronin and Dowsett, 1991). As summarized by Dowsett et al. (1994), this middle Pliocene interval is characterized by moderate to extreme (+2°C to more than +6°C) warming of surface waters in the middle- to high-latitude North Atlantic and North Pacific oceans, reduced polar ice sheets as implied by global sea levels that were 20–40 m above present levels, and major changes in the distributional patterns of vegetation in the Northern Hemisphere.

As part of the PRISM project, Barron (1992) completed detailed diatom paleoclimatic studies at Site 580 for the interval between 3.25 and 2.08 Ma (ages according to the Berggren et al. [1985] geomagnetic polarity time scale). Sample spacing averaged 11 k.y. between 3.1 and 2.8 Ma, but increased to 14–10 k.y. before 3.1 and after 2.8 Ma. Using a paleoclimate curve (*Twt*) based on the ratio of warm-water (subtropical) to cold-water diatoms with warm-water transitional taxa (*Thalassionema nitzschioides, Thalassiosira oestrupii,* and *Coscinodiscus radiatus*) factored into the equation at an intermediate (0.5) value, Barron (1992) argued that at least three times between 3.1 and 3.0 Ma paleotemperatures at Site 580 may have exceeded maximum Holocene values by 3°–5.5°C. In terms of the geomagnetic polarity time scale used for Leg 145 studies (Cande and Kent, 1992), this warm interval would fall between about 3.21 and 3.08 Ma, or roughly equivalent to the middle normal polarity event (C2An.2n) of the Gauss Normal-Polarity Chron and the lowermost part of the Kaena Reversed-Polarity Subchron of the Gauss Normal-Polarity Chron (C2Ar.1r).

Ocean Drilling Program (ODP) Leg 145 cored 25 holes at seven sites in a west to east transect of the subarctic North Pacific (Fig. 1). Three of these sites (882, 883, and 887) were cored on top of seamounts, where carbonate-bearing sediments relatively free of terrigenous debris offered the best possibility of high-resolution paleoceanographic studies. Site 884, on the east flank of the Detroit Seamount, was cored to obtain a comparative record of deep-sea sedimentation and to record the history of the Mejii sediment tongue. Site 881 was selected to be a northern extension of the south-to-north paleoceanographic transect begun off Japan during DSDP Leg 86 (Sites 578–580; Fig. 1), whereas Sites 885 and 886 were placed in the low-biologic-production central North Pacific where a good record of eolian deposition was expected (Rea, Basov, Janecek, Palmer-Julson, et al., 1993).

Diatoms are abundant and magnetostratigraphy is available for the Gauss Normal-Polarity Chron at all of these Leg 145 sites (Rea, Basov, Janecek, Palmer-Julson, et al., 1993; G. Dubuisson, written comm., 1993; Thiedemann and Haug, this volume), thus making them all prime targets for high-resolution paleoclimatic study.

The purpose of this paper is to complete high-resolution paleoclimatic diatom studies for the middle part of the Gauss normal polarity Chron (Subchrons C2Ar.1r through C2Ar.2r [Kaena through Mammoth Reversed-Polarity Subchrons]), or roughly 3.4–3.0 Ma at the Leg 145 sites.

MATERIALS AND METHODS

Because Sites 882–884 lie relatively close together on the Detroit Seamount in the northwest Pacific and because Site 886 is located only 2.2 km to the east of Site 885, only one site was selected for diatom paleoclimatic study from each of these two areas. Site 883 (Table 1) was chosen from the Detroit Seamount area because diatom pres-

[1] Rea, D.K., Basov, I.A., Scholl, D.W., and Allan, J.F. (Eds.), 1995. *Proc. ODP, Sci. Results,* 145: College Station, TX (Ocean Drilling Program).

[2] U.S. Geological Survey (MS 915), 345 Middlefield Road, Menlo Park, CA 94025, U.S.A.

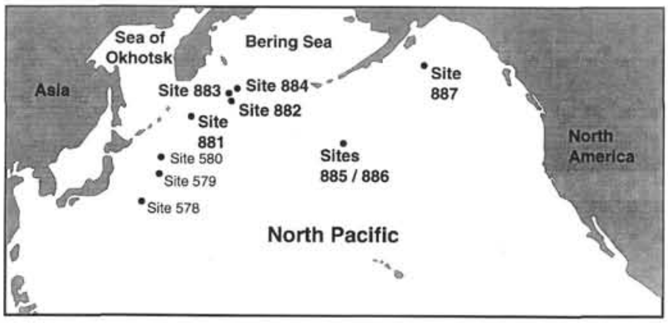

Figure 1. Location of ODP Sites 881–887 and DSDP Sites 578–580 in the North Pacific.

ervation there is better in the middle part of the Pliocene than it is at Site 884 and because the magnetostratigraphy available in the middle part of the Pliocene at Site 883 was of higher quality than what was available at Site 882. The decision to sample Site 885 (Table 1) rather than Site 886 was arbitrary; however, Dickens et al. (this volume) provide a detailed correlation of the two sites and show that they possess the same stratigraphic record. Sites 881 and 887 (Table 1) are sufficiently separated from the other Leg 145 sites to warrant individual study (Fig. 1).

Samples for high-resolution diatom paleoclimatic study of the middle part of the Pliocene (3.4–3.0 Ma; ages according to Cande and Kent [1992] geomagnetic polarity time scale) were taken from Sites 881, 883, 885, and 887 aboard the *JOIDES Resolution* and supplemented by additional samples taken at the Gulf Coast Repository. Sampling intervals were every 30 cm in Hole 881C (~10 k.y.); every 40 cm in Holes 883B and 883C (~3–4 k.y.), every 40 cm in Hole 885A (~40 k.y.), and every 20 cm in Holes 887A and 887C (~7–8 k.y.).

Samples were disaggregated in distilled water. The acid was then removed through several washings in distilled water separated by at least 4 hr of settling and decanting away of the liquid. The final sample was stored in a vial containing 7–10 times as much distilled water as sample. To prepare slides, the vial was shaken and a drop of the suspension was taken after 5–10 s from near the top of the vial, transferred to a 22 × 20 mm cover slip and allowed to dry overnight. Slides were then mounted in Hyrax (index of diffraction = 1.71). Whenever possible, at least 300 individual diatoms were counted using the counting techniques of Schrader and Gersonde (1978) by making random traverses of the slide under the light microscope at 1250×.

Counting categories follow those of Koizumi and Tanimura (1985), Sancetta and Silvestri (1986), and Barron (1992), which emphasize taxa that are most common and consistent. Following the advice of C. Sancetta (oral comm., 1990), *Actinocyclus ochotensis* and *A. oculatus* are considered to be either variants or ancestral relatives of *A. curvatulus* and are tabulated with that taxon. Similarly, forms that are tabulated as *Thalassiosira oestrupii* s. ampl. also include *T. tetraoestrupii* of Bodén (1993), and *Nitzschia reinholdii* s. ampl. also includes *N. marina*. The reader is referred to Akiba and Yanagisawa (1986) and Barron and Gladenkov (this volume) for taxonomic citations.

RESULTS

Sites 885 and 887

Light microscope examination of diatom assemblages from the middle part of the Pliocene of Sites 885 and 887 showed them to be overwhelmingly poorly preserved and not suitable for detailed paleoclimatic study. Typically, assemblages are quantitatively dominated by fragments of the robust diatom *Coscinodiscus marginatus*, indicating strong dissolution (Burckle et al., 1992). Although selected samples with better preservation may be suitable for study, it was decided to limit the present quantitative diatom studies to Sites 881 and 883. The reader is referred to Dowsett and Ishman (this volume) for detailed foraminifer paleoclimatic studies at Site 887, as well as at Site 883 using shared middle Pliocene sample sets.

Table 1. Latitude, longitude, and water depth of DSDP and ODP holes discussed.

Hole	Latitude (N)	Longitude	Water depth (m)
579A	38°37.61′	153°50.28′E	5737
580	41°37.47′	153°58.58′E	5375
881C	47°06.133′	161°29.490′E	5530.8
883B	51°11.908′	167°46.128′E	2395.6
883C	51°11.919′	167°46.123′E	2396.5
885A	44°41.296′	168°16.319′W	5708.5
887A	54°21.921′	148°26.765′W	3631.2

Site 881

Detailed sampling on board the ship for diatom studies was carried out in Hole 881C; however, the individual events of the Gauss Chron were only identified by shipboard magnetostratigraphy in Hole 881D (Shipboard Scientific Party, 1993a). Nevertheless, magnetic susceptibility events provide a means for a rather precise correlation between the two holes that allows absolute ages to be assigned to the samples from Hole 881D.

Table 2 lists the relative percentages of diatom taxa in Core 145-881C-21X. Referring to the core logs on pages 432 and 443 of Rea, Basov, Janecek, Palmer-Julson, et al. (1993), magnetic susceptibility peaks at 182.8 and 184.0 mbsf in the upper part of Core 145-881C-21X can be correlated with peaks recorded at 180.6 and 181.8 mbsf in the lower part of Core 145-881D-3H, suggesting a 2.2 m displacement of equivalent horizons between Holes 881C and 881D. Magnetic susceptibility peaks at 188.6 and 189.6 mbsf in the lower part of Core 145-881C-21X can be matched with peaks at 185.3 and 186.3 mbsf in the upper part of Core 145-881D-4H, which calls for a 3.3 m displacement of equivalent horizons between Holes 881C and 881D. An 8 cm thick ash layer corresponding to the deepest of these magnetic susceptibility peaks can also be correlated between the two holes. Thus, the onset of the Kaena Reversed-Polarity Subchron (3.127 Ma), which is identified at 181.50 mbsf in Core 145-881D-3H (Shipboard Scientific Party, 1993a), should occur at 183.70 mbsf in Core 145-881C-21X. Likewise, the termination and onset of the Mammoth Reversed-Polarity Subchron (3.221 and 3.325 Ma), which are found at 184.20 and 186.20 mbsf in Core 145-881D-4H, would appear to be present at 187.50 and 189.50 mbsf, respectively, in Core 145-881C-21X. Using these criteria, ages have been assigned to the diatom counts that have been completed for Core 145-881C-21X (Table 2). The interval studied in this core ranges in age from 3.399 to 3.085 Ma, with an average sample spacing of 10.5 k.y.

The diatom assemblage in Core 145-881C-21X is comparable with that documented in the middle part of the Pliocene at DSDP Site 580 by Barron (1992), with *Coscinodiscus marginatus* and *Neodenticula kamtschatica* as the dominant components and *Hemidiscus cuneiformis* as an important secondary component (Fig. 2). *Coscinodiscus marginatus* typically ranges in abundance from 10% to 40% of the assemblage; however, values of 46.8% and 56.4% are reached at 188.51 (3.274 Ma) and 186.42 (3.194 Ma) mbsf, respectively, where they may be enhanced by the dissolution of more delicate taxa (Burckle et al., 1992).

As at Site 580, relatively high values (8%–20%) of *H. cuneiformis* typify much of the section, especially at 3.32 Ma (16%) and between 3.21 and 3.09 Ma (Fig. 2). For comparison, relative percentages of *H. cuneiformis* range from 13% to 35% of the assemblage in the age-equivalent interval of Site 580. C. Sancetta (oral comm., 1992) has not recorded *Hemidiscus cuneiformis* in excess of 8% of the diatom assemblage in the numerous North Pacific core tops that she has studied, so the middle Pliocene abundance of *H. cuneiformis* in Holes 580 and 881C represents a non-modern analog situation. Sancetta (oral comm., 1992) suggests that higher numbers of *H. cuneiformis* in surface sediments are associated with the central subtropical gyre and are indicative of summer temperatures of at least 20°C. Maximum summer sea-surface temperatures today at the location of Site 881 are 12.3°C (Smith, 1991; Schweitzer, 1993), and it seems rather extreme to expect a +8°C warming of summer surface waters over Site 881 in the middle part of the Pliocene, especially as other tropical diatoms (*Azpeitia nodulifera, Nitzschia jouseae, N. reinholdii,* and *Thalassiosira convexa*) are relatively sparse during the same interval (Table 2).

The central subtropical gyre, where *H. cuneiformis* is most abundant in the modern ocean, however, is also characterized by relatively high salinities and nutrient-limited production; so it is possible that either or both of these factors may have also been responsible for increased abundances of *H. cuneiformis* during the middle part of the Pliocene at Sites 580 and 881. Based on the relatively high values of diatom flux (1.22 g/cm^3 k.y.) that are calculated for the middle Pliocene at Site 881 (Shipboard Scientific Party, 1993a), it seems unlikely that nutrients were limiting at that time to diatom production. On the other hand, increased salinities of surface waters in this middle latitude region of the North Pacific during the middle Pliocene might be expected if the Subarctic Front was weaker than at present, and saline, subtropical waters penetrated further to the north. In support of this hypothesis, Sancetta and Silvestri (1986) argue that before 2.5 Ma the modern subarctic water mass did not exist in the western Pacific and a broad transition zone extended from south of 41°N to north of 48°N was present in the North Pacific.

Neodenticula kamtschatica, a Pliocene ancestor of the subarctic form *N. seminae,* generally averages about 25%–30% of the middle Pliocene diatom assemblage of Site 881, although it increases to 50% or more of the assemblage in individual samples (Fig. 2). *Neodenticula kamtschatica* and *Coscinodiscus marginatus* appear to display opposite abundance trends. While these fluctuations may reflect changes in surface water characteristics, it is also possible that number of *C. marginatus* are enhanced in selected samples by increased dissolution (Burckle et al., 1992).

Thalassionema nitzschioides, which dominates the subtropical and warm transitional modern diatom assemblages of Sancetta and Silvestri (1986), generally constitutes <10% of the assemblage at Site 881 (Fig. 2), which contrasts with the higher values (>10%–53%) that were recorded by Barron (1992) at more southerly Site 580. *Actinocyclus curvatulus* and *Thalassiosira latimarginata,* taxa indicative of Sancetta and Silvestri's (1986) Sea of Okhotsk assemblage, together make up less than 10% of the middle Pliocene diatom assemblage of Site 881 (Table 2). Likewise, benthic diatoms and such displaced neritic taxa as *Actinoptychus* sp., *Paralia sulcata,* and *Stephanopyxis* species are quite rare.

Site 883

Site 883 (Table 1; Fig. 1), lies within the West Subarctic Gyre, which is one of four gyres that comprise the larger cyclonic Subarctic Gyre (Dodimead et al., 1963). The relative percentage of diatom taxa in the middle part of the Pliocene of Hole 883B is listed in Table 3. Ages for diatom samples (Table 3) are based on the paleomagnetic control for Hole 883B provided by G. Dubuisson (written comm., 1993), who estimates the respective onset and termination of the Mammoth Reversed-Polarity Subchron at 154.9 and 141.45 mbsf, and the respective onset and termination of the Kaena Reversed-Polarity Subchron at 133.9 and 125.15 mbsf in the hole.

Comparison of gamma-ray attenuation porosity evaluator (GRAPE) and magnetic susceptibility records (Shipboard Scientific Party, 1993b) indicate that sediments not recovered between Cores 145-883B-15H and 16H are represented by a 170-cm-long interval of Core 145-883C-16H (from Section 145-883C-16H-1, 110 cm, to -16H-2, 130 cm). These samples were also studied (Table 3), and their ages were estimated by interpolation. The paleomagnetic depth estimates of Dubuisson represent the midpoint between samples of inclination reversals, therefore, given Dubuisson's 1.5 m sampling interval and the approximate 130 m/m.y. sediment accumulation rate, an error of about ± 6 k.y. should be considered in estimating these ages.

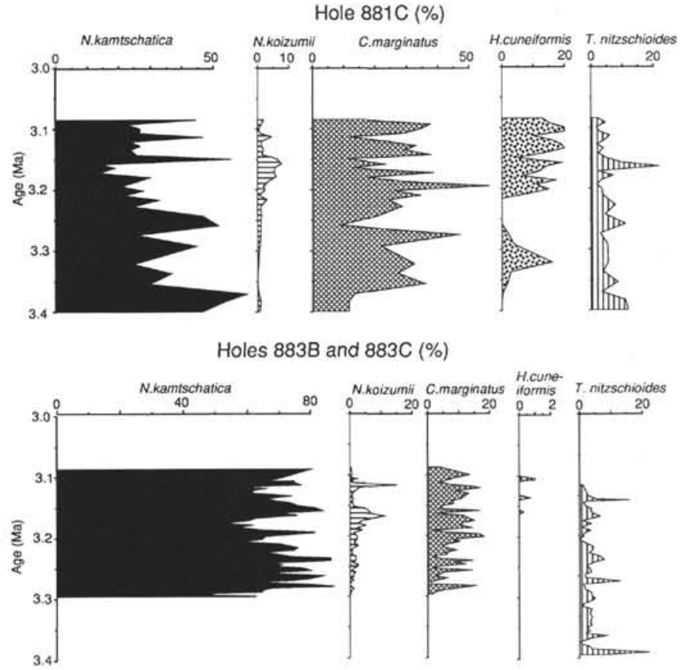

Figure 2. Comparison of the relative percent of *Neodenticula kamtschatica, N. koizumii, Coscinodiscus marginatus, Hemidiscus cuneiformis,* and *Thalassionema nitzschioides* in the middle part of the Pliocene of Hole 881C with that of Holes 883B and 883C.

The interval studied from Site 883 ranges in age from 3.296 to 3.087 Ma; the sampling interval (40 cm) corresponded to an average sample spacing of 3.6 k.y. *Neodenticula kamtschatica* is by far the most abundant diatom recorded, with relative percentages generally ranging from 60% to 85% of the total diatom assemblage (Table 3; Fig. 2). The related taxon, *N. koizumii,* is more or less consistently present in middle Pliocene assemblages of Site 883, but typically at relatively low percentages (<10%) compared to *N. kamtschatica.* As in Hole 881C, a small abundance peak of *N. koizumii* is present between about 3.17 and 3.15 Ma (Fig. 2).

Coscinodiscus marginatus is also an important constituent of the assemblage; however, it never totals more than 20% of the assemblage. These lower values at Site 883 relative to those recorded at Site 881 (Fig. 2) may be the result of better preservation of the diatom assemblages at the former site, which lies on the top of a seamount rather than on the seafloor. However, it also is possible that *C. marginatus* was less frequent in middle Pliocene surface waters to the north of the transitional zone, in the same manner as in the modern North Pacific (Sancetta and Silvestri, 1986).

In contrast to the data from Site 881, *Hemidiscus cuneiformis* is absent from most of the Site 883 samples. Where it does occur, it never constitutes more than 1% of the assemblage (Fig. 2). Other warm-water species (*Azpeitia nodulifera, Nitzschia fossilis, N. reinholdii* s. ampl., and *Thalassiosira convexa*) occur very sparsely (<1%) and sporadically in the middle Pliocene of Site 883. Site 883, therefore, was north of the region where *H. cuneiformis* was common during the middle Pliocene, as sampled at Sites 580 (Barron, 1992) and 881 (Fig. 2), and therefore north of the transition zone with subtropical waters. This observation supports the results of Sancetta and Silvestri (1986), who concluded that the Pliocene transition zone in the North Pacific was rather broad before 2.5 Ma, possibly extending from 41° to 48°N.

Table 2. Relative percentage of diatom taxa vs. age in Hole 881C for the middle part of the Pliocene.

Core, section, interval (cm)	Depth (mbsf)	Age (Ma)	*Actinocyclus curvatulus*	*Actinocyclus octonarius*	*Actinoptychus* spp.	*Astl.* and *Astp.* spp.	*Azpeitia nodulifera*	*Azpeitia tabularis*	*Actinopcyclus ellipticus*	*Chaetoceros* spores	*Coscinodiscus marginatus*	*Hemidiscus cuneiformis*	*Neodenticula kamtschatica*	*Neodenticula koizumii*	*Nitzschia cylindra*	*Nitzschia fossilis*	*Nitzschia jouseae*	*Nitzschia reinholdii* s. ampl.	*Nitzschia* spp.	*Paralia sulcata*	*Pyxidicula zabelinae*	*Rhizosolenia* spp.	*Simonseniella barboi*	*Stellarima* spp.	*Stephanopyxis* spp.	*Thalassionema nitzschioides*	*Thalassiosira convexa*	*Thalassiosira eccentrica*	*Thalassiosira jacksonii*	*Thalassiosira latimarginata*	*Thalassiosira leptopus* s. ampl.	*Thalassiosira nidulus* s. ampl.	*Thalassiosira oestrupii* s. ampl.	*Thalassiosira* spp.	*Thalassiothrix longissima*	Other	Benthic diatoms	Total count
145-881C-																																						
21H-1, 25–25	181.95	3.085	2.2	0.3	0.3					1.2	16.1	12.7	44.6	1.9					0.2			0.6	1.5		0.3	2.2	0.3			1.2	5.0		1.5	0.9	6.2	0.6		323
21H-1, 51–52	182.21	3.092	0.7			0.7				0.7	37.6	14.9	23.1	1.3				0.3			0.3				0.3	4.6			1.3		4.6		1.3	1.3	6.9			303
21H-1, 81–82	182.51	3.099	0.7							0.3	34.7	20.5	26.7	0.3								1.0	0.7			1.7		0.3	0.7		4.0		1.0	1.0	6.6			303
21H-1, 116–117	182.86	3.106	1.7			0.3	0.3	0.3		1.0	29.5	19.5	27.5	0.7		0.3		0.3				0.3			0.3	2.6					1.7		0.3	1.3	11.3	0.7		302
21H-1, 141–142	183.11	3.113	1.6			0.6			0.3	1.0	11.9	10.3	47.3	4.5		0.3		0.3	1.9			0.6			0.3	6.1			0.6		2.9		2.3	1.9	5.1			311
21H-2, 22–23	183.42	3.120	0.3	0.6		0.3				0.3	24.4	15.9	23.8	1.3		0.6		2.5				0.3	1.0		0.3	4.4					6.0		0.3	0.6	16.5	0.3		315
21H-2, 51–52	183.71	3.127	0.9							0.6	33.0	18.6	27.0	1.3				0.3	0.3		0.3					1.9					5.7		0.9	1.3	7.5	0.3		318
21H-2, 81–82	184.01	3.134	0.7			0.3				1.3	29.8	20.2	24.2	2.0				1.0	0.7			0.7	0.3		0.7	4.0	0.7	0.3			3.0		1.0	1.7	7.6			302
21H-2, 116–117	184.36	3.142				1.0				3.0	37.6	12.9	26.2	1.5					0.5			1.0	1.0			2.5	1.0		1.0		3.0				5.4	2.0		101
21H-2, 141–142	184.61	3.149	0.7							0.7	11.5	4.9	55.9	6.3				0.3	0.3			1.6	1.0		0.3	4.6	0.7	0.7			2.3		1.6	1.6	3.3	0.7	1.0	304
21H-3, 22–23	184.92	3.157	1.7	1.0		0.7				0.7	23.2	18.9	14.9	7.6					0.7			1.7	0.3		0.3	9.6	0.3	0.3			6.6		4.0	2.3	4.3	0.3	0.7	302
21H-3, 51–52	185.21	3.164	1.0	0.3	0.3		0.7	0.3	0.3	0.3	12.6	13.6	18.9	5.6				2.7				0.3	1.0	0.3	1.0	22.3	1.7		0.7	0.3	2.7		2.7	2.3	6.6	1.3		301
21H-3, 81–82	185.51	3.172	2.0								38.6	11.9	14.4	5.4				2.0						1.0		2.5	5.0		2.0		5.0			3.0	7.4			101
21H-3, 116–117	185.86	3.179	1.3				1.6			1.0	17.7	6.6	30.2	5.9				0.7	0.3			1.6	0.3		0.3	7.2	1.3		0.7	0.3	4.6		6.6	3.6	7.9		0.3	305
21H-3, 141–142	186.11	3.186	0.3	0.3			0.3			0.3	29.5	17.4	25.6	3.3				0.3			0.3			0.3		3.3	3.6				3.9		2.3	2.3	6.2	0.3		305
21H-4, 22–23	186.42	3.194	1.0								56.4	10.9	20.8	2.0												2.0					3.0			1.0	3.0			101
21H-4, 51–52	186.71	3.201	1.0			0.3				2.3	26.5	14.6	28.5	2.3			0.3	0.6	0.3			0.3	1.6			3.6	1.6	0.3	0.3	0.3	3.9		0.6	1.9	8.7			309
21H-4, 81–82	187.01	3.209	3.5						0.5	0.5	34.3	8.0	21.9	0.5						0.5		0.5	1.0			3.7	2.5	0.5	0.5		6.0		4.5	1.5	9.0	0.5		201
21H-4, 116–117	187.36	3.216	1.5	0.5							24.3		32.7	3.0			1.2	0.5	0.5				1.5			5.0	2.0		0.5		6.9		7.9	5.4	5.4	1.0		202
21H-4, 141–142	187.61	3.227	2.0	1.0		1.0				4.0	28.7		24.8	1.0				1.0				1.0			1.0	7.9	4.0	1.0	2.0		4.0		5.0	4.0	6.9			101
21H-5, 22–23	187.92	3.243	2.6		0.3					2.6	20.9		47.4	1.3			0.3		0.3	0.3		0.7			0.3	4.6	1.7		0.3		5.0		4.3	2.0	4.6		0.3	302
21H-5, 51–52	188.21	3.258	1.7	0.3	0.3					2.6	8.9		51.8	1.0		0.3		1.7				0.3				10.9	0.7		1.0	1.0	5.3	0.7	3.0	2.3	5.0	1.3		303
21H-5, 81–82	188.51	3.274	0.5							3.0	46.8	2.0	25.9	1.0				1.5	0.5		0.5		1.5			3.0	1.0				4.0			1.5	7.0	0.5		201
21H-5, 116–117	188.86	3.292	2.3							0.7	22.0	3.9	44.7	0.7		0.3		1.3		0.3		1.0	0.3			5.3	1.6		0.3		3.3		1.0	2.3	7.9	0.3	0.3	304
21H-6, 22–23	189.42	3.321	2.0							0.7	32.5	16.2	25.2	0.3			0.7	0.3		0.3	1.3	0.7	1.0			5.6	0.3				1.7		0.3	1.0	9.9			302
21H-6, 51–52	189.72	3.336	1.9								27.2	2.9	36.9					1.0	1.0	2.9			2.9			3.9					3.9		1.9	1.9	11.7			103
21H-6, 86–87	190.06	3.354	1.0		2.0	1.0				1.0	36.0	2.0	30.0				0.5				3.0		1.0		1.0	8.5					3.0		1.0	3.0	6.0			100
21H-6, 116–117	190.36	3.370	0.7							4.3	13.5	0.3	60.5	0.3				0.2			0.3	2.3	0.3	0.3		3.6		0.3		0.3	5.6	0.3	1.0	2.0	3.3	0.3		304
21H-6, 141–142	190.62	3.383	0.7							1.7	11.6		54.0	1.0	0.7							1.3	0.3	0.7	0.3	10.6				2.6	7.3	0.3	2.0	2.3	2.6			302
21H-7, 23–24	190.93	3.399	2.3							2.3	11.8		47.1	0.7				0.7	0.3	0.3		1.0	0.3	0.3	3.9	12.4		1.0	0.7	2.6	3.6	0.3	2.6	1.3	3.9	0.7		306

Table 3. Relative percentage of diatom taxa vs. age in Holes 883B and 883C for the middle part of the Pliocene.

Core, section, interval (cm)	Depth (mbsf)	Age (Ma)	*Actinocyclus curvatulus*	*Actinocyclus octonarius*	*Actinoptychus* spp.	*Astl.* and *Asp.* spp.	*Azpeitia nodulifera*	*Azpeitia tabularis*	*Bacteriosira fragilis*	*Chaetoceros* spores	*Coscinodiscus marginatus*	*Hemidiscus cuneiformis*	*Neodenticula kamtschatica*	*Neodenticula koizumii*	*Nitzschia cylindra*	*Nitzschia fossilis*	*Nitzschia grunowii*	*Nitzschia reinholdii* s. ampl.	*Nitzschia* spp.	*Paralia sulcata*	*Rhizosolenia* spp.	*Simonseniella barboi*	*Stellarima* spp.	*Stephanopyxis* spp.	*Thalassionema nitzschioides*	*Thalassiosira convexa*	*Thalassiosira eccentrica*	*Thalassiosira jacksonii*	*Thalassiosira latimarginata*	*Thalassiosira leptopus* s. ampl.	*Thalassiosira nidulus*	*Thalassiosira oestrupii* s. ampl.	*Thalassiosira* spp.	*Thalassiothrix longissima*	Other	Benthic diatoms	Total count
145-883B-																																					
14H-6, 90–95	130.30	3.087	1.3								4.0		80.1	0.3					0.3		0.3			0.7	1.0		0.3		7.0			0.7	2.6	1.3			302
14H-6, 136–141	130.76	3.100	1.0			0.3				1.3	13.3		72.3	0.7			0.3				1.0				2.7		0.3		3.0	0.3		0.7	1.0	1.0	0.7		300
14H-7, 25–30	131.15	3.104	0.3							1.7	10.3	1.0	69.2								1.3			1.0	5.3		0.3		3.0	0.3		0.7	1.0	2.6	2.0		302
14H-7, 65–70	131.39	3.106	1.0			0.7				1.3	6.5	1.0	61.1	2.3							0.7			0.7	16.0				3.6	0.7		1.3	0.7	2.0	0.7		306
15H-1, 5–10	131.45	3.107	0.7							0.7	7.5	0.3	74.5	0.3	0.3						0.7			0.7	2.6		0.3		5.9			0.7	2.0	1.6	1.0	0.3	306
15H-1, 45–50	131.85	3.109	1.0			0.7				0.3	5.6		74.8	1.0								0.3		0.3	1.3		1.0		3.7	1.0		2.3	2.3	4.0	0.3		301
15H-1, 85–90	132.25	3.113	1.0			1.0		0.3		0.3	4.0		76.9	0.7							0.3			0.3	2.0		0.7		2.6	0.3		0.3	1.3	7.6	0.3		303
15H-1, 125–130	132.65	3.116	0.7			0.3				1.0	7.6		56.1	15.3					0.3		1.0	0.3		0.7	3.7				5.0	0.3		2.0	2.3	2.7	0.7		301
15H-2, 15–20	133.05	3.119	1.0	0.3		1.0				1.0	14.2		65.2	4.6											3.6				2.3	0.7		1.7	1.7	2.0	0.7		302
15H-2, 51–56	133.41	3.122	0.7			0.7				1.0	16.7		62.1	2.6								0.3		1.3	4.2		0.7		2.0	2.3		1.6	1.0	2.3	0.3	0.3	306
15H-2, 91–96	133.81	3.126	3.6	0.3		1.6				0.3	9.1		61.6	1.6							1.3	0.3		0.7	6.5		0.3	0.3	1.6	1.6		3.3	2.3	2.3	1.0	0.3	307
15H-2, 135–140	134.25	3.131	1.0							0.7	13.2		73.4	0.7					0.7		0.3			0.7	1.0				2.6	0.7		1.3	2.3	0.7	0.7	0.3	304
15H-3, 25–30	134.65	3.135	0.3			0.7				1.0	11.6	0.7	66.1	0.7		0.7			0.3			1.0		0.7	3.7		1.0		1.3	2.0	0.3	2.0	2.3	2.7	0.7	0.3	301
15H-3, 65–70	135.05	3.139	0.7			1.0				1.3	10.9		69.4	1.0					0.7		0.7			0.3	0.7		1.0		2.0	1.3	0.3	2.3	2.0	3.3	0.3	1.0	304
15H-3, 102–107	135.42	3.143	0.3			0.7					7.6		73.6	0.7					0.3		0.7				3.6		0.3		0.7	1.0		3.6	3.0	2.6	0.7	0.7	303
15H-3, 145–150	135.85	3.147								3.0	8.3		76.3	1.0					0.7		0.3			0.7	1.3		0.7		0.7	1.3		2.0	1.0	2.7			300
15H-4, 35–40	136.25	3.151			0.3	0.7				1.7	4.6		81.8	1.0			0.3			0.3	0.3				1.3		0.3		1.0	0.3		2.0	1.3	0.7	1.3	0.7	302
15H-4, 75–80	136.65	3.155									4.3		84.2	5.3			0.7				0.3					0.3	1.0		1.0			1.7	0.7		0.3	0.3	303
15H-4, 111–116	137.01	3.159	0.3			0.7				0.7	16.8	0.3	67.7	6.3										0.3	2.0		0.3		0.3	0.3		1.7	1.3	1.0			303
15H-5, 5–10	137.45	3.163	1.0							1.0	2.0		76.2	6.6					0.3		0.7			0.3	4.3				2.3	0.7		1.0	1.0	1.7	0.7	0.3	303
15H-5, 46–51	137.86	3.167	1.3			0.3			0.3	0.3	11.6		63.1	10.6					0.3		1.0			1.0	4.3				2.0	1.0		1.7	0.7	0.7			301
15H-5, 86–91	138.26	3.171	1.3			1.0				0.3	12.9		60.6	7.3			0.3		0.3		0.7			1.0	3.0	0.7	0.3		2.0	2.0		2.3	2.0	1.3		0.7	302
15H-5, 126–131	138.66	3.175	2.6		0.3	0.3				3.0	14.9		52.1	4.0					0.3		2.0				6.6	0.3	0.3		1.7	3.3		1.3	3.0	4.0			303
15H-6, 15–20	139.05	3.179	1.0		0.3	1.0				2.0	11.2		60.9	2.6			0.3		0.7			1.6			7.9	0.3	0.3	0.3	0.7	3.3		0.3	2.3	2.0	0.7	0.3	304
15H-6, 50–55	139.40	3.183	2.3		0.7	1.3				3.3	10.4		57.3	4.9					0.3		0.7			0.3	4.6	0.7	0.7	0.3	1.0	4.6		2.3	2.3	1.6	0.3	0.3	307
15H-6, 91–96	139.81	3.187	1.3			0.7				3.0	13.9		64.7	2.3		0.3			0.3					1.0	2.3	0.3	1.0		1.0	3.6		0.3	3.0	1.0			303
15H-7, 35–40	140.25	3.191	0.3							2.3	1.7		82.0	4.0	0.3				0.3		0.7				3.3	0.3	0.7			0.7		1.3	1.0	0.7	0.3		300
15H-7, 66–71	140.56	3.195	1.0			0.3				3.0	6.0		73.3	1.3			0.3		0.7		0.3	0.3		0.3	3.7	0.3	1.3		0.7	0.7		2.3	2.3	0.7	0.3	0.7	300
145-883C-																																					
16H-1, 125–130	137.25	3.197				0.3	0.3			3.3	16.6		66.1	1.7							0.3			0.3	1.7	1.0	0.3		1.3	3.3		1.0	0.7	1.3		0.3	301
16H-2, 15–20	137.65	3.202	0.7							0.3	17.9		65.2	2.3					0.3		0.7			0.7	2.0				0.3	5.6		0.7	2.0	0.7	0.7		302
16H-2, 55–60	138.05	3.206	0.7			0.3				5.9	8.3		57.1	2.3	0.3				0.3		0.7				12.9		0.3		0.3	4.3		2.0	0.7	2.3	0.3	1.0	303
16H-2, 95–100	138.45	3.210	2.0			0.7				3.3	10.3		70.0	1.3							1.3			0.3	1.3				1.0	2.3		1.7	2.0	2.3			300
145-883B-																																					
16H-1, 5–10	140.95	3.216	0.3			0.3				3.0	4.6		76.2	2.6					0.7		0.3	0.7		0.3	1.7		0.7		1.0	0.7		1.3	2.3	3.3			303
16H-1, 45–50	141.35	3.220	0.3		0.3	0.7				1.3	5.6		75.4	1.0					0.3		0.3				3.7				1.0	3.0		2.7	2.3	1.7	0.3		301
16H-1, 85–90	141.75	3.224	2.0		0.3	0.3				2.0	9.3		65.2	0.7					0.3		0.3	0.3			4.0		1.7			3.6		2.6	3.6	3.3	0.3		302
16H-1, 125–130	142.15	3.228	0.7			0.3				1.3	5.6		71.3	0.7							0.7			0.3	5.0		1.3			2.0		3.3	2.3	4.0	0.7	0.7	303
16H-2, 15–20	142.55	3.231			0.3					1.3	6.3		73.7	0.7					0.3		1.3	0.3		0.3	3.3		1.3	0.3	1.0	3.6	0.3	2.0	2.6	0.7		0.3	304
16H-2, 50–55	142.90	3.234				0.3				1.0	2.0		86.8	2.0					0.3		0.3				1.3		0.3			0.7		2.6	0.7	1.0	0.3	0.3	302
16H-2, 90–95	143.30	3.237	1.0							0.3	3.3		86.8	2.0					0.3			0.3		0.3	1.0				0.3	1.0		0.7	1.7	1.0			303
16H-2, 135–140	143.75	3.241	1.0		0.3					1.3	14.6		65.6	2.0					0.3		0.7				4.0				0.7	4.0		2.0	1.3	2.0		0.3	302
16H-3, 25–30	144.15	3.244	0.7			0.7				0.7	9.2		71.2	0.7								0.3			3.3		1.0	0.3		2.6		3.3	3.3	2.6		0.3	306
16H-3, 65–70	144.55	3.247				0.7				1.7	12.0		69.1	2.7	0.3		0.3				0.3			1.7	3.3		0.7		1.0	1.7		1.0	2.3	1.3			301
16H-3, 101–106	144.91	3.250	0.7							1.0	4.0		77.9	2.6			0.3				0.3			0.7	4.0		0.7		1.0	0.7		2.0	2.3	1.7		0.3	303
16H-3, 145–150	145.35	3.254	0.3							1.0	1.6		79.6	1.0						0.3	0.3			0.3	3.6		2.6		1.3	2.3		0.3	3.0	2.0		0.3	304
16H-4, 35–40	145.75	3.257	1.0							1.0	14.5		64.7	0.7							0.3	0.7			3.3		2.3		0.7	3.6		2.3	2.6	2.0	0.3		303
16H-4, 75–80	146.15	3.260	0.3		0.3	0.3					5.6		73.9	2.0		0.3			0.3					0.3	4.0		2.0		1.3	3.6		1.3	3.0	1.0	0.3		303
16H-4, 111–116	146.51	3.263								0.3	4.3		83.7	1.0					0.3	0.3					2.3		0.3		1.3	1.3		1.3	2.0	1.3			301
16H-5, 5–10	146.95	3.267	0.7			0.3	0.3			2.0	2.6		80.1	1.3					0.3		0.7	0.3		0.3	3.3		1.0		1.0	0.7		1.6	2.0	1.3		0.3	306
16H-5, 45–50	147.35	3.270	0.7			0.3				1.3	6.3		75.5						0.3		0.7	0.7		0.3	2.0		1.7		1.3	0.7		1.7	3.0	2.6	1.0		302
16H-5, 85–90	147.75	3.273	0.7					0.3		3.0	4.0		60.0	1.3							0.3	0.7		0.3	8.7		2.3			1.3		6.3	3.0	7.7			300
16H-5, 120–125	148.10	3.276	0.3			0.3				0.7	1.0		77.9	0.3							1.7			0.3	3.3		1.0		1.7	4.0		2.6	2.3	2.3	0.3		303
16H-6, 15–20	148.55	3.280	0.3					0.3		0.3	1.3		87.9								0.3				0.3		0.7		0.7	1.6		1.3	3.0	1.3	0.7		305
16H-6, 50–55	148.90	3.283	0.7			1.0				0.7	15.9		68.1						0.3		0.7	0.3		1.3	0.7		0.3		0.7	3.3	0.3	0.7	3.0	1.3	0.3	0.3	301
16H-6, 90–95	149.30	3.286	1.0							0.3	10.5		65.1	1.3			0.3				3.0		0.7	0.7	3.0		1.0	0.3	1.6	5.9		1.6	3.3	0.3			304
16H-6, 135–140	149.75	3.289	2.0							1.7	5.9		65.0	0.7					0.3		1.7	0.3	0.7	3.3	4.0		1.7		2.3	4.0	0.3	1.7	2.6	1.7	0.3		303
16H-7, 25–30	150.15	3.293	1.3		0.3	0.3				5.6	2.6		36.8	0.3	0.3		2.6		0.3		5.0	0.3		1.3	22.2		1.7		1.3	5.0		6.0	4.0	2.0	0.7		302
16H-7, 64–69	150.54	3.296	0.7		0.3		0.3			3.3	1.7		63.1	0.3	0.7		0.3				0.7		0.7	3.0	7.3		2.0		1.7	5.6		5.3	1.0	1.7	0.3		301

As at Site 881, *Thalassionema nitzschioides* generally comprises <10% of the middle Pliocene diatom assemblage of Site 883; except for values of 22.2%, 12.9%, and 16.0% in samples dated at 3.293, 3.206, and 3.104 Ma, respectively (Table 3; Fig. 2). This is in contrast to Site 580 to the south, where Barron (1992) recorded *T. nitzschioides* relative abundance values in excess of 30% in numerous samples of the middle Pliocene.

Similarly, the Sea of Okhotsk diatoms, *Actinocyclus curvatulus* and *Thalassiosira latimarginata,* constitute a comparably small proportion of the middle Pliocene diatom assemblage of Site 883 (together, <10%), as was found at Site 881 (Tables 2, 3). Diatoms indicative of sea ice (*Nitzschia cylindra* and *N. grunowii*) display sparse and sporadic occurrences; the maximum abundance of *N. grunowii* only comprises 2.6% of the assemblage at 150.15 mbsf (3.293 Ma). Benthic diatoms and displaced neritic taxa, such as *Actinoptychus* spp., *Paralia sulcata,* and *Stephanopyxis* spp., are also quite rare in the middle Pliocene at Site 883, although *Stephanopyxis* spp. constitutes about 3% of the assemblage in samples dated at 3.289 and 3.296 Ma.

DIATOM PALEOCLIMATIC CURVES

Twt

For a paleoclimatic study of DSDP Site 580, Barron (1992) introduced the diatom paleoclimatic ratio, *Twt.*

$$Twt = (X_w + 0.5X_t)/(X_c + X_t + X_w),$$

where X_w equals subtropical to tropical taxa (*Azpeitia nodulifera, A. tabularis, Actinocyclus ellipticus, Hemidiscus cuneiformis, Nitzschia reinholdii* s. ampl., *N. fossilis, N. jouseae,* and *Thalassiosira convexa*); X_t equals warm transitional taxa (*Coscinodiscus radiatus, Thalassionema nitzschioides,* and *Thalassiosira oestrupii*); and X_c equals the total percentage of cold-water taxa (*Actinocyclus curvatulus, Neodenticula koizumii, N. kamtschatica, Chaetoceros* spores, *Simonseniella [Rhizosolenia] barboi, Thalassiosira latimarginata,* and *Coscinodiscus marginatus*). Barron (1992) argued that the *Twt* ratio looked promising for Pliocene paleoclimatic studies, because *Twt* values were typically highest for the most southerly DSDP Site 578, intermediate for intermediate Site 579, and lowest for northern Site 580.

On Figure 3, *Twt* curves that have been derived for the middle Pliocene of Sites 881 and 883 are compared with Barron's (1992) *Twt* curve for Site 580 (ages updated to the Cande and Kent [1992] geomagnetic polarity time scale) and with the benthic foraminiferal oxygen isotope curve of Shackleton et al. (1995) for equatorial Pacific Site 846. As observed by Barron (1992) at DSDP Sites 578–580 to the south, the middle Pliocene *Twt* curves for DSDP Site 580 and Holes 881C and 883B consistently display a south-to-north decrease in values (i.e., they decrease relative to sea-surface temperature) for any given age. The curve for Holes 883B and 883C is relatively flat, with *Twt* values consistently below 0.1, as one might expect from the northern position of Site 883 (51°12′N) and the overwhelming subarctic character of its diatom assemblages (Fig. 2). The Hole 881C curve displays some of the same trends as the curve for Site 580, but it is consistently offset by 0.4–0.2 *Twt* units below that of the more southerly site, possibly reflecting a surface-water temperature gradient between the two sites. The Site 580 curve rises to maximum "warm peak" values between about 3.21 and 3.05 Ma, whereas the Hole 881C curve peaks in the middle of this same period (at about 3.16 Ma). Higher *Twt* values in these intervals are the result of greater relative percentages of *Hemidiscus cuneiformis* in the Site 580 and Hole 881C assemblages (Barron, 1992, and Fig. 2).

The Site 846 isotope curve displays relatively light interglacial values (~3.1‰) during the mid Gauss interval from 3.3 to 3.05 Ma, while glacial values, with the exception of event KM2, are typically less than or equal to modern interglacial values (3.4‰) (Shackleton et al., 1995). A rough correlation between interglacial and glacial events in the isotope data and warm and cold peaks, respectively, in the Site 580 *Twt* curve seems apparent from Figure 3; however, the Site 580 data lack both the temporal resolution and the precise correlation with the oxygen isotope curve that are needed to establish such relationships.

Paleotemperature Estimates

Because modern core-top data was unavailable to Barron in 1992 and because the *Twt* ratio uses numerous extinct Pliocene species, Barron (1992) stated that there was no direct way to estimate paleotemperatures with the *Twt* ratio. Recently, however, Constance Sancetta (written comm., 1994) has distributed her original diatom assemblage data on 216 cores from the North Pacific, Sea of Okhotsk and Bering Sea. Within the northwest quadrant of the North Pacific (32° to 53°N; 143° to 180°E), which includes Sites 580, 881, and 883, assemblage data is available on 51 piston cores.

Although precise sea-surface temperature preferences are not available for extinct diatom species such as *Neodenticula kamtschatica, N. koizumii,* and *Nitzschia reinholdii,* extensive Pliocene assemblage data provides a basis for assessing the paleoclimatic preferences of these taxa (Koizumi, 1985; Barron, 1992). *Neodenticula kamtschatica* and *N. koizumii* are known to be ancestors of the modern subarctic form *N. seminae,* and fossil assemblage data suggest they had a similar distribution. Likewise, *Simonseniella barboi* is a known ancestor of the Pleistocene cool-water diatom *S. curvirostris,* and appears to have had similar ecological preference (Koizumi, 1985; Sancetta and Silvestri, 1986).

The living tropical to subtropical taxon *Fragilariopsis doliola* is a known descendant of the fossil form *Nitzschia fossilis,* whereas *Nitzschia reinholdii* is closely related to the modern subtropical to tropical form, *N. marina.* Pliocene assemblage data strongly suggest that these fossil taxa occupied a similar warm-water niche to that of their relatives. Similarly, the extinct Pliocene diatoms, *Thalassiosira convexa* and *Nitzschia jouseae,* were clearly also warm-water forms based on their relative abundances at Sites 578–580 (Koizumi, 1985), 580 (Barron, 1992), and 881 and 883 (Tables 2, 3).

Assuming these paleoclimatic preferences, a correspondence between Pliocene and modern *Twt* ratios might also be inferred; and it should be possible to use modern core-top data to suggest possible Pliocene paleotemperatures for Sites 580, 881, and 883.

Figure 4 compares modern *Twt* indices for the 51 northwest Pacific core-top assemblages (data from C. Sancetta, written comm., 1994) with modern August and February sea-surface temperature (SST) data (after Schweitzer, 1993). Whereas a strong linear relationship (R^2 = 0.807) exists between *Twt* and February SST, a much weaker relationship (R^2 = 0.594) is apparent between *Twt* and August SST.

On Figure 5 the linear regression equations of Figure 4 have been used to plot estimated February and August SSTs for the middle part of the Pliocene of Sites 580, 881, and 883. Between about 3.21 and 3.05 Ma, February SSTs at Site 580 are estimated to have averaged about 7°C above the modern value of 5.3°C. At Site 881, maximum February SSTs of about 6°C above modern values are suggested for the interval between about 3.18 and 3.08 Ma. During the same period of time at northern Site 883, *Twt* ratios suggest that February SSTs were near modern (1.5°C) values.

Predicted August SSTs for the same intervals of time are all above modern values at the three sites: +2°–3°C (Site 580), about +6°C (Site 881), and about +5°C (Site 883). Because the linear relationship between *Twt* and August SST is rather weak, these estimated SSTs are considered to be doubtful.

Td_f

Because the relatively high numbers of *Hemidiscus cuneiformis* at Sites 580 and 881 strongly affect the *Twt* ratios and because such high abundances of this taxon may represent a non-modern analog situation, it may be advisable to use an alternative climate ratio to *Twt* to suggest paleotemperatures. At the same time, use of a climate ratio that compares diatoms of similar size and resistance to dissolution should reduce any bias in sample preparation techniques (Laws, 1983) and sample preservation.

One approach would be to compare relatively small, finely silicified pennate taxa of contrasting paleotemperature preference. In terms of the Pliocene assemblages, *Nitzschia reinholdii* s. ampl., which includes *N. marina* and displays a warm-water temperature preference, could be compared with *Neodenticula* spp. (*N. koizumii* and *N. kamtschatica*), which prefer cooler waters. These taxa are easily recognized and have a similar resistance to dissolution (Mikkelsen, 1980).

Ratios of the modern representatives of these groups, *Nitzschia marina* and *Neodenticula seminae,* were determined for the northwest Pacific core-top data set and compared with modern SST data. A strong linear relationship ($R^2 = 0.749$) was revealed between the *N. marina* to (*N. marina* + *N. seminae*) ratio with February SSTs, while a much weaker relationship ($R^2 = 0.486$) with August SSTs was apparent (Fig. 6).

Factoring *Thalassionema nitzschioides* into this equation at one half the value of *Nitzschia marina,* markedly improves the linear relationships with both February and August SSTs. According to Mikkelsen (1980), *T. nitzschioides* has a similar moderate resistance to dissolution as does *N. marina* and *Neodenticula* spp. Figure 7 compares the relationships of a ratio of *N. marina* + 0.5 × {*T. nitzschioides*} to total *N. marina* + *T. nitzschioides* + *Neodenticula seminae.* The resulting R^2 values increase to 0.888 and 0.736 for February and August SSTs, respectively.

Consequently, a climate ratio, Td_f, is proposed, where $Td_f = (X_{Nr} + 0.5 \times \{X_{Tn}\})/(X_{Nr} + X_{Tn} + X_{Neo})$ and X_{Nr} = *Nitzschia reinholdii* s. ampl. (including *N. marina*), X_{Tn} = *Thalassionema nitzschioides,* and X_{Neo} = the total *Neodenticula* spp.

On Figure 8, the linear regression equations comparing modern Td_f ratios to February and August SSTs (Fig. 7) have been used along with calculated Td_f ratios for Sites 580, 881, and 883 (data of Barron, 1992, and Tables 1 and 2) to suggest Pliocene SST estimates for the three sites. In the middle Pliocene interval of study, the Td_f ratios suggest that February SSTs averaged about 4°–5°C above modern values at Site 580; while at Site 881, they fluctuated from about 0° to 5°C above modern values. Near modern (or slightly colder) February SSTs are suggested for Site 883. As to estimated August SSTs, the Td_f ratios predict the following deviations from modern values during the middle part of the Pliocene: +2°C to +3°C at Sites 580 and 881 and +4°C at Site 883.

Comparison of SST Estimates

At Site 580 Barron (1992) suggested a maximum warming of +3°C in the summer and +5.5°C in the winter above modern values during interglacial periods dated between about 3.2 and 3.1 Ma. The new August SST estimates of +2°–3°C for both the *Twt* and Td_f ratios at Site 580 are consistent with Barron's (1992) estimate, while the new estimated February SSTs of +7°C (*Twt*) and +4°–5°C (Td_f) are both warmer and slightly cooler than Barron's (1992) estimate. Because the *Twt* ratio at Sites 580 and 881 is strongly affected by high numbers of *Hemidiscus cuneiformis* that greatly exceed values in the modern ocean, the Td_f-derived SST estimate is preferred.

Correspondingly, at Site 881 mid-Pliocene SSTs for August are considered to have also been 2°–3°C above modern values, while those for February SSTs appear to have fluctuated between 0°C and 5°C above modern values (Td_f-derived estimates).

For northern Site 883, both climate ratios suggest little or no change from modern February SSTs during the middle part of the Pliocene; however, for August slightly greater warming (+4°C to +5°C above modern values) is suggested at Site 883 than what is estimated at Sites 580 and 881 (+2°C to +3°C).

On Karaginsky Island (58.85°N, 164.04°E) off Kamchatka Gladenkov et al. (1993) use middle Pliocene molluscan assemblages to suggest February SSTs were +4°C above modern values, while August

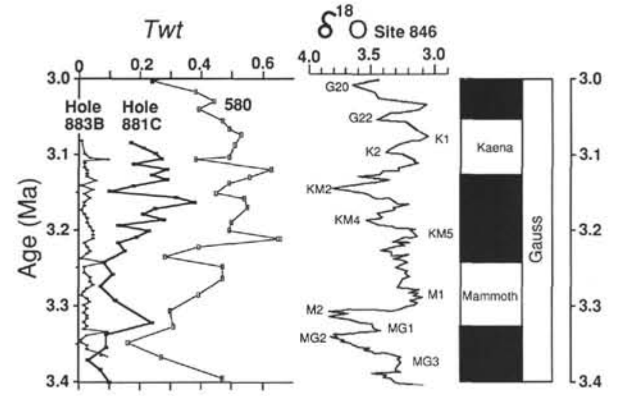

Figure 3. Comparison of Barron's (1992) diatom paleoclimatic ratio *Twt* for Sites 883, 881, and 580 with Shackleton et al.'s (1995) benthic foraminifer oxygen isotope curve for Site 846 in the eastern equatorial Pacific. Shackleton et al.'s (1995) oxygen isotope curve has been shifted slightly with respect to age to conform to the Cande and Kent (1992) time scale.

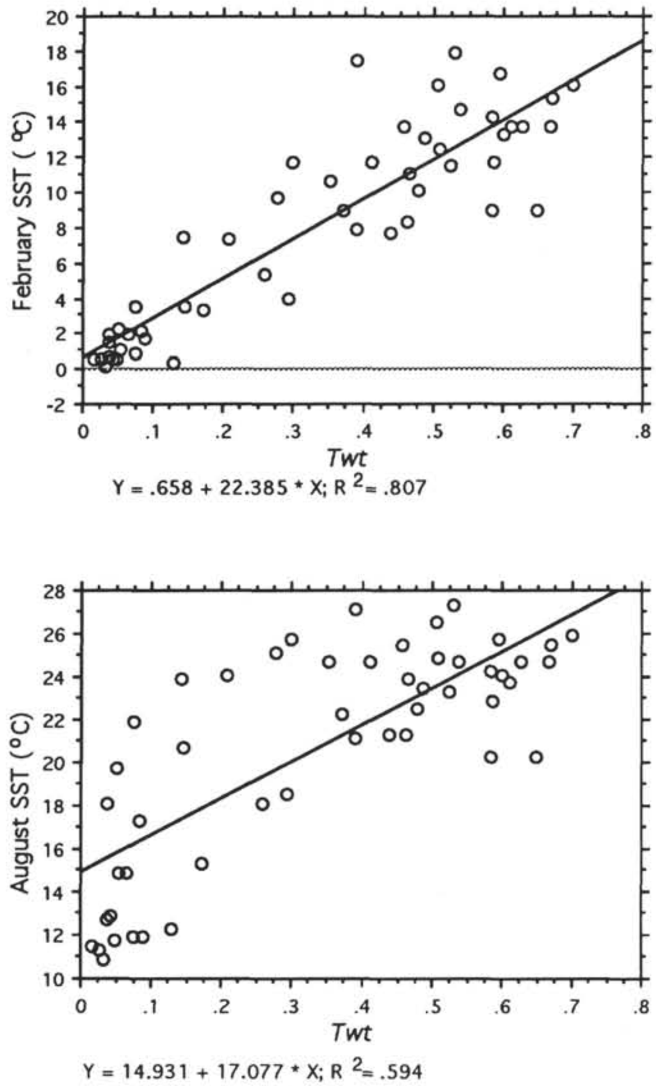

Figure 4. Linear regression plots of the *Twt* paleoclimate ratio in northwest Pacific core-top assemblages (data from C. Sancetta, written comm., 1994) vs. modern February and August sea-surface temperatures (SSTs).

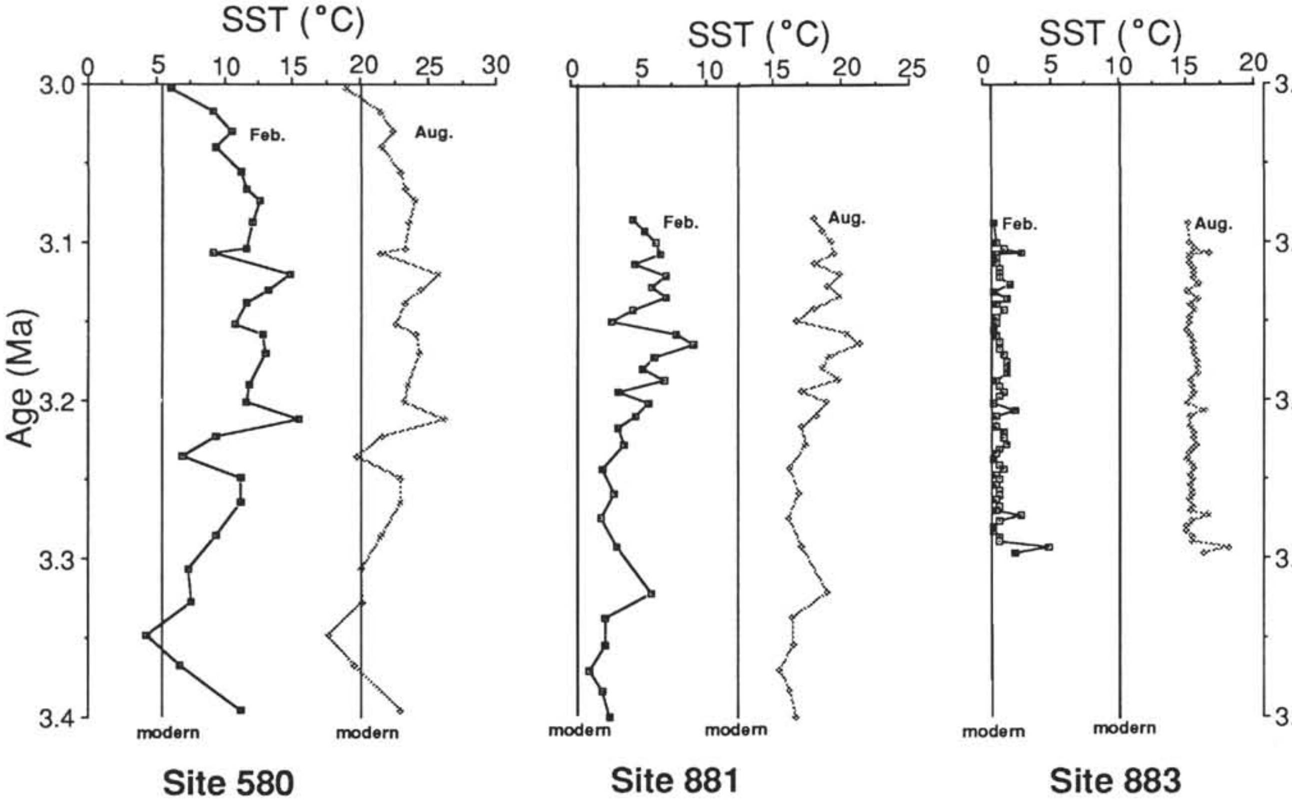

Figure 5. Estimated February and August SSTs for the middle part of the Pliocene at Sites 580, 881, and 883 derived from the *Twt* ratios and the linear regression equations of Figure 4. Modern SSTs at the various sites are indicated by a vertical line.

SSTs were only 2°C warmer than modern values. This contrasts with a greater warming (+4°C to +5°C) predicted by diatoms for August vs. February (little or no change) at Site 883. However, Cronin et al. (1993) also argue for more warming relative to present (+4°C) in August vs. February (+2°C) in a 3 Ma Colvillian exposure in Alaska at 70.29°N, 150.42°W based on ostracode data. Dowsett et al. (1994) argue that during the middle part of the Pliocene, greater August warming compared to February warming is the rule in the middle latitude (37° to 56°N) northeastern Atlantic, where it probably reflects greater northward heat transport of surface waters during the summer months.

CONCLUDING REMARKS

At Site 881 middle Pliocene (~3.4–3.1 Ma) diatom assemblages are dominated by *Coscinodiscus marginatus* and *Neodenticula kamtschatica,* with a significant contribution from *Hemidiscus cuneiformis.* Although higher (>40%) relative abundances of *C. marginatus* may be the result of dissolution, *C. marginatus,* a probable cool-transitional to subarctic form, and *N. kamtschatica,* a probable subarctic diatom, shift back and forth as the dominant species, possibly reflecting changes in surface water characteristics. Relative abundance values of *Hemidiscus cuneiformis,* a modern subtropical diatom, are highest (typically 10%–20% of the assemblage) during the same 3.20 to 3.08 Ma interval; an isolated value of 16.2% for *H. cuneiformis* also occurs at about 3.32 Ma. High percentages of *H. cuneiformis* (13%–35% of the assemblage) occur during the same time interval (3.21–3.07 Ma) at the more southerly DSDP Site 580. These increases in the abundance of *H. cuneiformis* (Fig. 2) argue for warming of the surface waters above Sites 580 and 881. Comparable middle Pliocene diatom assemblages at Sites 580 and 881 support the conclusion of Sancetta and Silvestri (1986) that before 2.5 Ma, a broad transition zone between subarctic and subtropical waters extended in the North Pacific from south of 41°N to north of 48°N.

At Site 883, the overwhelming dominance of *Neodenticula kamtschatica* in the middle Pliocene diatom assemblages and predicted February SSTs that are near modern values are taken as evidence that Site 883 remained within the Pliocene equivalent of a subarctic water mass throughout the middle Pliocene interval from 3.3 to 3.09 Ma. August SSTs are estimated to have been +4°C (Td_f) to +5°C (*Twt*) above modern values, possibly reflecting greater surface water equator-to-pole heat transport during the summer.

Comparison of modern *Twt* ratios for 51 core-top diatom assemblages from the northwest Pacific with modern February and August sea-surface temperature (SST) data reveals a strong linear relationship between *Twt* and February SSTs (R^2 = 0.807), while a much weaker (R^2 = 0.594) relationship is apparent between *Twt* and August SSTs. Using a linear regression equation for *Twt,* middle Pliocene to modern anomalies for February SSTs are estimated to have been about +7°C at Site 580 (3.21–3.05 Ma); about +6°C at Site 881 (3.18–3.08 Ma); and about +1°C at Site 883 (3.3–3.1 Ma).

An alternative climate ratio, Td_f, is proposed, where $Td_f = (X_{Nr} + 0.5 \times \{X_{Tn}\})/(X_{Nr} + X_{Tn} + X_{Neo})$ and X_{Nr} = *Nitzschia reinholdii* s. ampl., X_{Tn} = *Thalassionema nitzschioides,* and X_{Neo} = the total *Neodenticula* spp. For modern core-top data, the Td_f ratio displays a strong linear relationship with both February and August SST data (R^2 = 0.888 and 0.736, respectively). Using the Td_f ratio, middle Pliocene to modern anomalies for February SSTs are estimated to have averaged +4°C to +5°C at Site 580 and about +0°C to +3°C at Site 881; near modern February SSTs (1°–2°C) are inferred for Site 883. Regarding August SSTs, the Td_f ratios predict +2°C to +3°C warming above modern values during the middle part of the Pliocene at Sites 580 and 881.

ACKNOWLEDGMENTS

The author is very grateful to Constance Sancetta for providing a copy of her modern core-top assemblage data. An earlier version of this paper benefited from the reviews of Eileen Hemphill-Haley, Harry Dowsett, Per Bodén, and Constance Sancetta. The comments of Constance Sancetta were especially helpful in revising the manuscript. Scott Starratt of the U.S. Geological Survey also provided editorial comments. Useful discussions with Lloyd Burckle are also acknowledged. Kevin Purcell of the U.S. Geological Survey provided assistance with sample preparation. The Ocean Drilling Program provided the samples studied. This paper is a product of the U.S. Geological Survey PRISM project.

REFERENCES*

Akiba, F., and Yanagisawa, Y., 1986. Taxonomy, morphology and phylogeny of the Neogene diatom zonal marker species in the middle-to-high latitudes of the North Pacific. *In* Kagami, H., Karig, D.E., Coulbourn, W.T., et al., *Init. Repts. DSDP,* 87: Washington (U.S. Govt. Printing Office), 483–554.

Barron, J.A., 1992. Pliocene paleoclimatic interpretations of DSDP Site 580 (NW Pacific) using diatoms. *Mar. Micropaleontol.,* 20:23–44.

Berggren, W.A., Kent, D.V., and Van Couvering, J.A., 1985. The Neogene: Part 2. Neogene geochronology and chronostratigraphy. *In* Snelling, N.J. (Ed.), *The Chronology of the Geological Record.* Geol. Soc. London Mem., 10:211–260.

Bodén, P., 1993. Taxonomy and stratigraphic occurrence of *Thalassiosira tetraoestrupii* sp. nov. and related species in upper Miocene and lower Pliocene sediments from the Norwegian Sea, North Atlantic and northwest Pacific. *Terra Nova,* 5:61–75.

Burckle, L.H., Sturz, A., and Emanuele, G., 1992. Dissolution and preservation of diatoms in the Sea of Japan and the effect on sediment thanatocoenosis. *In* Pisciotto, K.A., Ingle, J.C., Jr., von Breymann, M.T., Barron, J., et al., *Proc. ODP, Sci. Results,* 127/128, Pt.1: College Station, TX (Ocean Drilling Program), 309–316.

Cande, S.C., and Kent, D.V., 1992. A new geomagnetic polarity time scale for the Late Cretaceous and Cenozoic. *J. Geophys. Res.,* 97:13917–13951.

Cronin, T.M., and Dowsett, H.J., 1991. Pliocene climates. *Quat. Sci. Rev.,* 10:115–296.

Cronin, T.M, Whatley, R.C., Wood, A., Tsukagoshi, A., Ikeya, N., Brouwers, E.M., and Briggs, W.M., Jr., 1993. Microfaunal evidence for elevated mid-Pliocene temperatures in the Arctic Ocean. *Paleoceanography,* 8:161–173.

Dodimead, A.J., Favorite, F., and Hirano, T., 1963. Salmon of the North Pacific, II—Review of the oceanography of the subarctic Pacific region. *Bull. Int. N. Pac. Fisheries Comm.,* 13:1–195.

Dowsett, H.J., Thompson, R.S., Barron, J.A., Cronin, T.M., Ishman, S.E., Poore, R.Z., Willard, D.A., and Holtz, T.R., Jr., 1994. Paleoclimatic reconstruction of a warmer earth: PRISM middle Pliocene Northern Hemisphere synthesis. *Glob. Planet. Change,* 9:169–195.

Gladenkov, Y.B., Barinov, K.B., Basilian, A.E., and Cronin, T.M., 1991. Stratigraphy and paleoceanography of Pliocene deposits of Karaginsky Island, eastern Kamchatka, USSR. *Quat. Sci. Rev.,* 10:239–246.

Kanaya, T., and Koizumi, I., 1966. Interpretation of diatom thanatocoenoses from the north Pacific applied to a study of core V20-130 (studies of a deep-sea Core V20-130, part IV). *Sci. Rep. Tohoku Univ., Ser. 2,* 37:89–130.

Koizumi, I., 1985. Late Neogene paleoceanography in the western north Pacific. *In* Heath, G.R., Burckle, L.H., et al., *Init. Repts. DSDP,* 86: Washington (U.S. Govt. Printing Office), 429–438.

Koizumi, I., and Tanimura, Y., 1985. Neogene diatom biostratigraphy of the middle latitude western North Pacific, Deep Sea Drilling Project Leg 86. *In* Heath, G.R., Burckle, L.H., et al., *Init. Repts. DSDP,* 86: Washington (U.S. Govt. Printing Office), 269–300.

Laws, R.A., 1983. Preparing strewn slides for quantitative microscopical analysis: a test using calibrated microspheres. *Micropaleontology,* 29:60–65.

Mikkelsen, N., 1980. Experimental dissolution of Pliocene diatoms. *Nova Hedwigia Beih.,* 23:893–911.

Rea, D.K., Basov, I.A., Janecek, T.R., Palmer-Julson, A., et al., 1993. *Proc. ODP, Init. Repts.,* 145: College Station, TX (Ocean Drilling Program).

Sancetta, C., and Silvestri, S., 1986. Pliocene–Pleistocene evolution of the North Pacific ocean-atmosphere system, interpreted from fossil diatoms. *Paleoceanography,* 1:163–180.

Schrader, H.-J., and Gersonde, R., 1978. Diatoms and silicoflagellates. *In* Zachariasse, W.J., Reidel, W.R., Sanfilippo, A., et al. (Eds.), *Micropaleontological Counting Methods and Techniques: An Exercise of an Eight Metres Section of the Lower Pliocene of Cap Rossello, Sicily.* Utrecht Micropaleontol. Bull., 17:129–176.

Schweitzer, P.N., 1993. Modern average global sea-surface temperature. *U.S. Geol. Surv. Digital Data Ser.,* DDS-10.

Shackleton, N.J., Hall, M.A., and Pate, D., 1995. Pliocene stable isotope stratigraphy of Site 846. *In* Pisias, N.G., Mayer, L.A., Janecek, T.R., Palmer-Julson, A., and van Andel, T.H. (Eds.), *Proc. ODP, Sci. Results,* 138: College Station, TX (Ocean Drilling Program), 337–356.

Shipboard Scientific Party, 1993a. Site 881. *In* Rea, D.K., Basov, I.A., Janecek, T.R., Palmer-Julson, A., et al., *Proc. ODP, Init. Repts.,* 145: College Station, TX (Ocean Drilling Program), 37–83.

————, 1993b. Site 883. *In* Rea, D.K., Basov, I.A., Janecek, T.R., Palmer-Julson, A., et al., *Proc. ODP, Init. Repts.,* 145: College Station, TX (Ocean Drilling Program), 121–208.

Smith, E., 1991. A user's guide to the NOAA Advanced Very High Resolution Radiometer Multichannel Sea Surface Temperature data set produced by the University of Miami/Rosenstiel School of Marine and Atmospheric Science. Distributed Active Archive Center, Jet Propulsion Laboratory, Pasadena, CA.

* Abbreviations for names of organizations and publications in ODP reference lists follow the style given in *Chemical Abstracts Service Source Index* (published by American Chemical Society).

Date of initial receipt: 5 April 1994
Date of acceptance: 1 August 1994
Ms 145SR-102

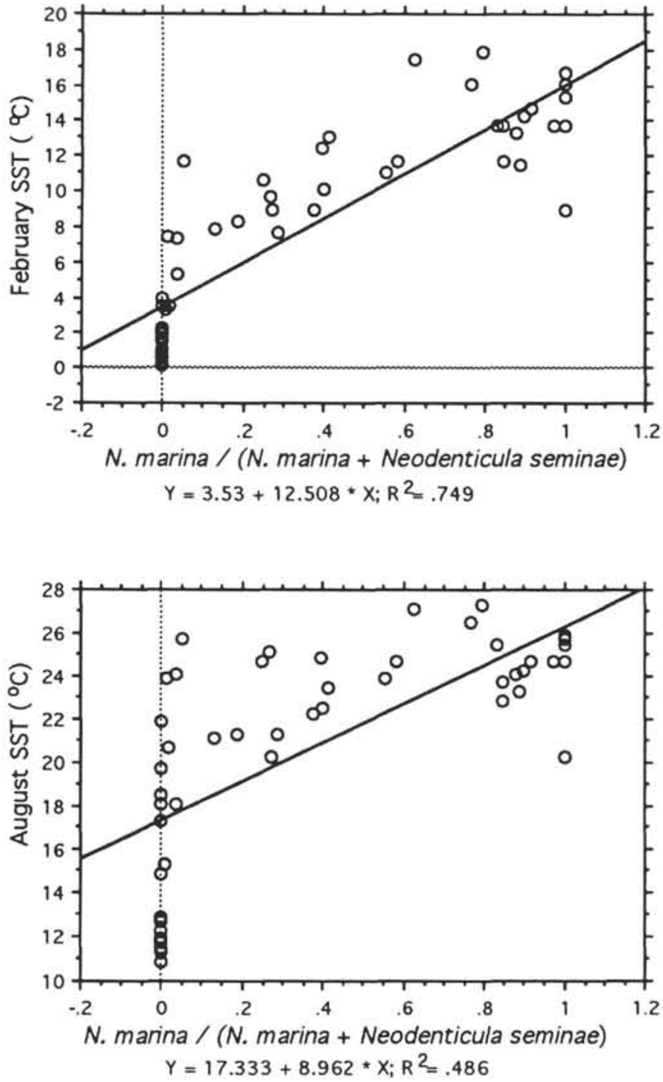

Figure 6. Linear regression plots of a ratio of *Nitzschia marina* to total *N. marina* + *Neodenticula seminae* in northwest Pacific core-top assemblages (data from C. Sancetta, written comm., 1994) vs. modern February and August sea-surface temperatures (SSTs).

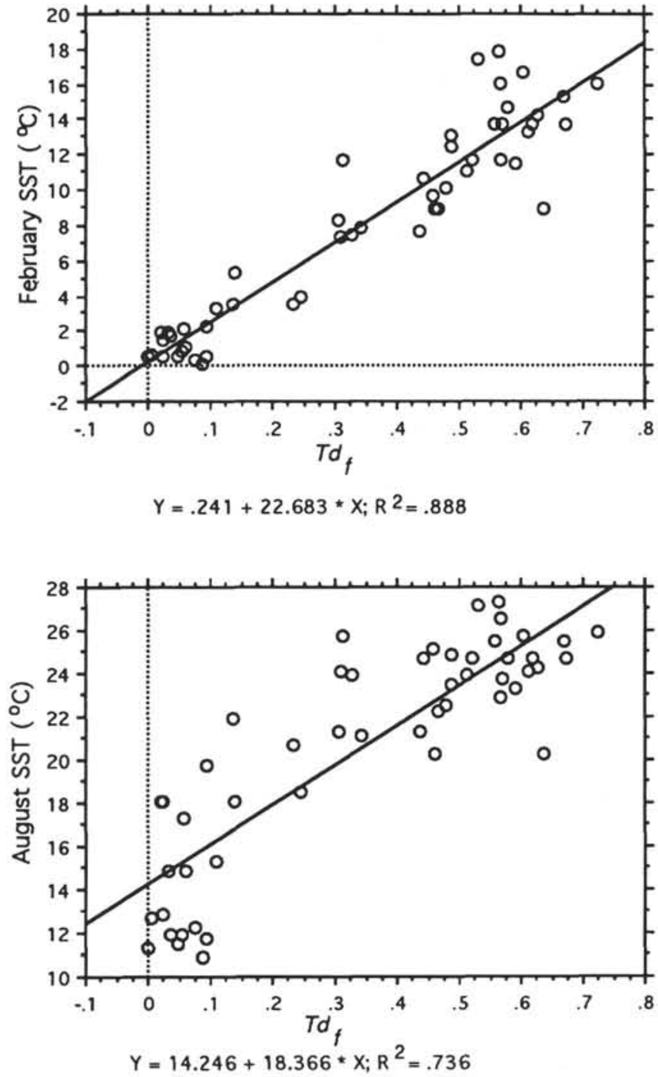

Figure 7. Linear regression plots of the Td_f paleoclimate ratio in northwest Pacific core-top assemblages (data from C. Sancetta, written comm., 1994) vs. modern February and August sea-surface temperatures (SSTs). $Td_f = (X_{Nr} + 0.5 \times \{X_{Tn}\})/(X_{Nr} + X_{Tn} + X_{Neo})$ and X_{Nr} = *Nitzschia reinholdii* and *N. marina*, X_{Tn} = *Thalassionema nitzschioides*, and X_{Neo} = the total *Neodenticula* spp.

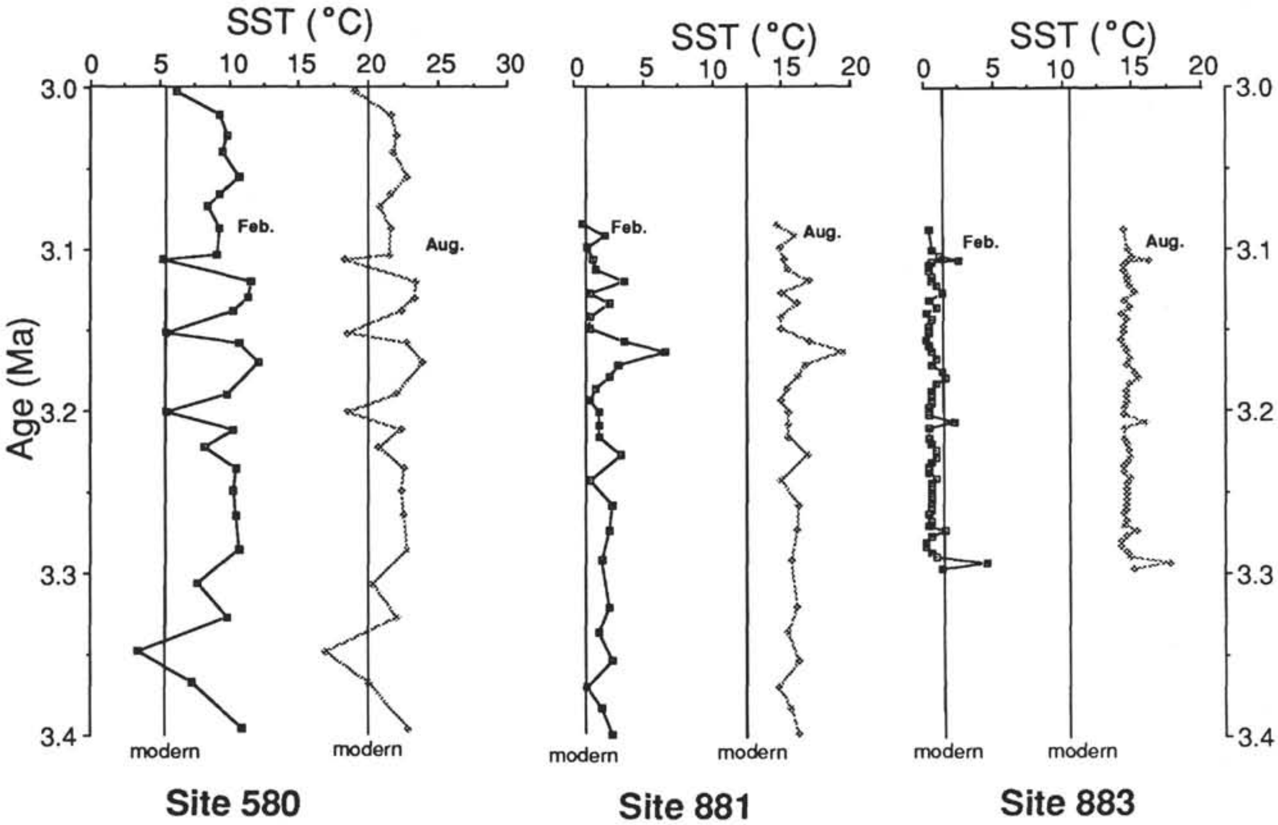

Figure 8. Estimated February and August SSTs for the middle part of the Pliocene at Sites 580, 881, and 883 derived from the Td_f ratios and the linear regression equations of Figure 7. Modern SSTs at the various sites are indicated by a vertical line.